ISSN No:-2456-2165

Development of Enriched Biochar from Local Materials by Mixture Design Approach

HASSANA Boukar*, DESOBGO ZANGUE Steve Carly*
University Institute of Technology (UIT)
P. O. Box 455. 455 Ngaoundere, Cameroon,

NGASSOUM Martin
National School of Agro-Industrial Science (ENSAI),
University of Ngaoundere P. O. Box 455, Ngaoundere, Cameroon,

BARKA Abakoura
Polytechnic University of Mongo, Chad

Abstract:- The aim of the study was to produce enriched Biochar from local materials. The mixture design enabled to model and optimize the production of a high-quality enriched biochar to be used as a bio fertilizer and/or a pollutant adsorbent. The choice was laid on three components bearing different attributes. These include lignocellulosic material (Ayous' sawdust); a minerals source material (the clay of Wak) and a nitrogen source material (chicken manure). The three responses associated to this study were the pH, the iodine index and the cation exchange capacity. The optimization consisted in the inquiry of a maximum compound desirability. The mathematical model reveals a quadratic type for all responses. The pH and the cation exchange capacity were highly influenced by the chicken manure component, the iodine index by the sawdust component. The optimization revealed a pH preview value of 9.25 for desirability of 0.96, an iodine index of 794 $m^2.g^{-1}$ for a desirability of 0.83, and a cation exchange capacity of 40.96 $cmol^+.kg^{-1}$ for the desirability of 0.97. The global desirability of 0.96 showed that all components reach a favorable result, hence guaranteed the use of such biochar as bio fertilizer and/or as pollutant adsorbent.

Keywords:- *Enriched biochar; sawdust; clay, chicken manure; mixture design, optimization.*

I. INTRODUCTION

Although the performance of classical biochar in the field of bioremediation of soils polluted with heavy metals(Pan et al., 2021; Yang et al., 2021)and in the fertilization of poor soils is well established(Li et al., 2018; Sun et al., 2021)there are still concerns with its economic profitability. A return on investment is not possible because of the use of large quantities of conventional biochar. In fact, it usually takes more than 5-30 t ha^{-1}(Blackwell et al., 2010; Chan, K.Y., Zu, 2009; Kimetu et al., 2008)to achieve desirable results.(Clare et al., 2015) and (Blackwell et al., 2015)estimated the cost of biochar production at about $ 300 t^{-1} in China and Australia, and at this price, the use of conventional biochar is not cost-effective. Since then, researchers and manufacturers have joined forces to develop another type of biochar i.e., the enriched biochar(Wang et al., 2017). The enriched biochar is supposed to have higher performances than the classical biochar. In addition, enriched biochar enhances the properties of soils even at low application doses. Among the most frequent soil properties are the pH, the specific surface, cation exchange capacity, water retention, immobilization of heavy metals, the increase of microflora and organic matter etc. (Cheng and Lehmann, 2009; Chia Bhupinder et al., 2014; Glaser et al., 2001; Joseph et al., 2010; Kimetu et al., 2008). If the main component of enriched biochar is generally a lignocellulosic material, secondary components such as iron oxide rich nanoparticles (Chen et al., 2011; Joseph et al., 2013), mineral-rich clays or nitrogen-rich animal'sexcreta (Cheng and Lehmann, 2009; Liang et al., 2006)are known to increase the performance of enriched biochar even atlowerquantities compared to conventional biochar. However, the choice of enriched biochar components and their proportions remain unjustified for most publications (Blackwell et al., 2015; Joseph et al., 2015; Li et al., 2017; Yao et al., 2014). The aim of this study is therefore to use amixturedesignas a tool to produce enriched biochar from locally available materials in the Cameroonian city of Ngaounderethat will enable to justifythe different component proportions. The optimization permit to obtain the optimal mixture that could be used in various applications such as the depollution of heavy metals polluted soils (Adjia et al., 2009; Noubissié et al., 2016); or as a biofertilizer on poor soils (Fezeu Wombuwou, 2006) of Ngaoundere.

II. MATERIAL AND METHODS

A. Sampling of raw materials

Three raw materials, namely *Ayous* sawdust, raw clay and chicken manure were chosen to serve as a basis for obtaining the three constituents of the mixture (Figure 1). The sawdust from *Triplochition scleroxylon*, locally known as *Ayous*or known as "white wood" was identified and collected in the sawmills of the city of *Ngaoundéré*, *Adamawa* region (Cameroon). These woodcutting residues in smaller flow is available in large quantities in the city of *Ngaoundere*(Hassana et al., 2019). The sawdust from this species is known to be a good generator of pores (Belibi Belibi, 2016; Rumaizah et al., 2019). The raw clay comes from the locality of Wak, a village located in the Adamawa region. The geographic coordinates of the sampling area are as follows: Latitude North N = 07°40'685''; Longitude East

ISSN No:-2456-2165

E = 013°33’026’’; Altitude H = 708m. Raw clay is readily available because it occupies a large surface area. Chicken manure are excrement produced by laying hens raised without litter on a farm in Ngaoundere. Poultry was fed mainly on corn. Just like the two raw materials chosen, chicken manure is widely available because poultry farming is developed in this area.

B. Pretreatment of the raw materials to obtain the constituents of the mixture

The pretreatment of the sawdust is done by drying the samples identified as being from the Ayous specie in ambient air for 48 hours in order to get rid of the moisture and facilitate the grinding process. The grinding is carried out using a grinder called "*Moulin d'Or*" rotating at 100 rpm. Screening using a sieve mesh less than or equal to 1000 microns allowed to obtain the sawdust powder (Figure 1, photo a). It is kept away from moisture for later use.

In order to obtain a pure clay powder (Figure 1, photo b), Wak raw clay is subjected to some treatments. A mass of 10 kg of clay is soaked in 20 liters of distilled water for 24 hours to defragment the different parts. A sieve with a mesh of 100 microns servestoobtain particles less than or equal to this mesh. The settling that ensued allowed to obtain a pellet. The latter is introduced into the oven for evaporation at 105 ° C until complete drying. Mortar grinding and re-sieving using a 100 µm mesh ends the pretreatment. The pretreatment of the manure consisted of drying the samples in ambient air for 72 hours in order to get rid of moisture. Manual sorting followed by sieving allowed separation of the chicken manure from other collected constituents such as litter or pebbles. Mortar grinding and sieving using a sieve with a mesh size of 100 µm allow to obtain the chicken manure powder (Figure 1, photo c).

Photo **a**: Sawdust powder from Ayous

Photo **b**: Wak Clay Powder

Photo **c**: Chicken manure powder

Fig. 1: Components of the enriched biochar. Process for producing enriched biochar

Fig. 2 shows the process for obtaining the enriched biochar. It is adapted from(Yao et al., 2014).

ISSN No:-2456-2165

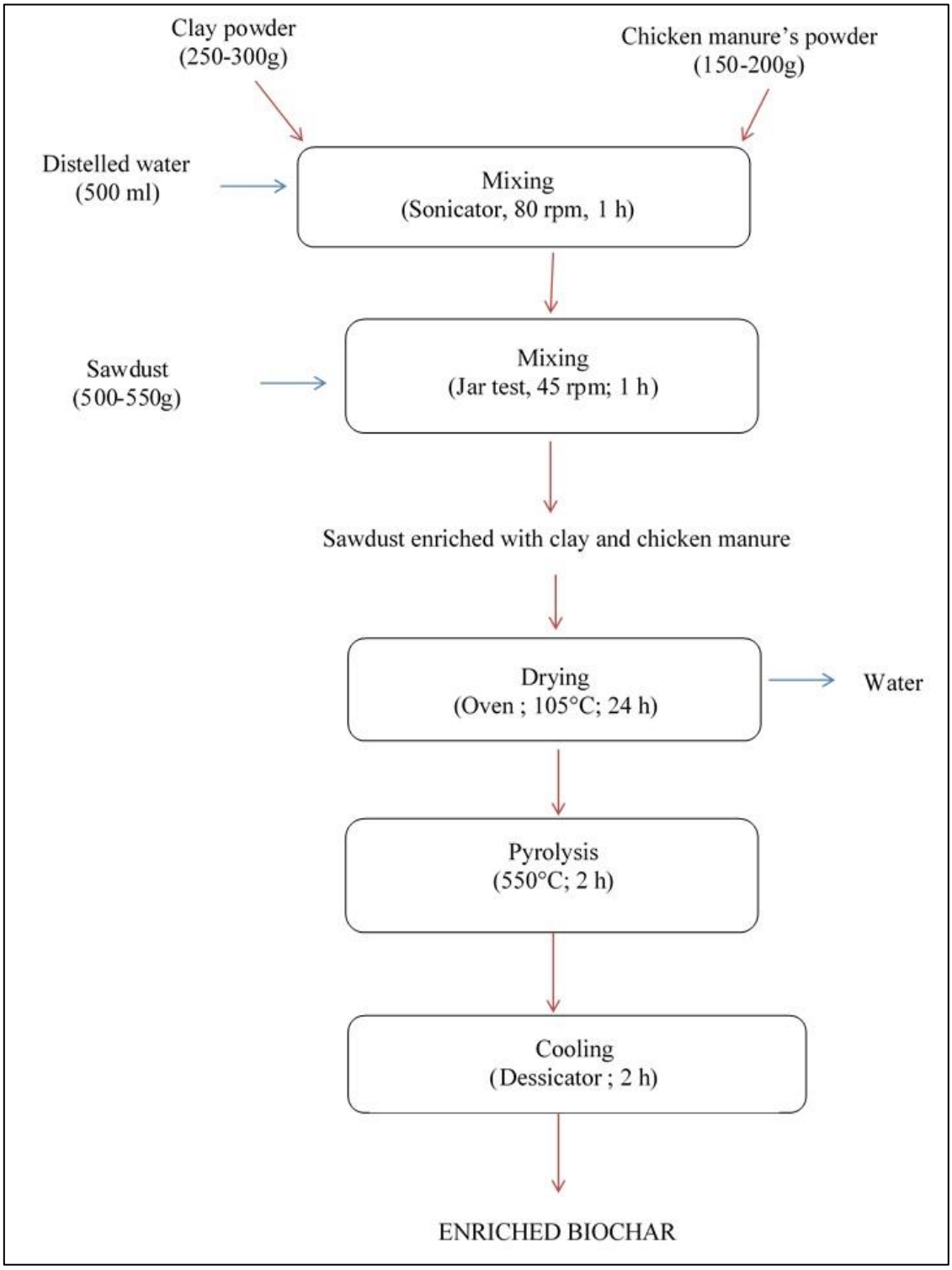

Fig. 2: Process schema for obtaining enriched biochar.

Different quantities of clay powder (250-300g) and chicken manure powder (150-200g) are manually mixed in 500ml of distilled water and then placed in a sonicator (*Brand Bransonic* 221, Danbury, USA). United). The mixture is stirred at 80 rpm for 60 minutes to be dispersed and homogenized. The mixture is then collected and placed in a basin. Various quantities of sawdust powder (500-550g) are added gradually and then mixed manually before being placed in a test jar to further mix and increase the homogenization of the three components. The shaking of the test jar (45 rpm) is also performed for 60 minutes. The mixture, which is an enrichment of the sawdust with the powdered clay and the chicken manure, is then placed in an oven at 105 ° C for 24 hours to remove the water thereby facilitating the pyrolysis. The mixture is placed in an oven for 2 hours at a temperature of 550 ° C. The *NAGAT* brand oven (France) with the characteristics (T ° C max: 950 ° C, Power: 6300 W, Max volume: 3 dm3) serves as a pyrolyzer. The enriched biochar obtained is cooled in a desiccator for 2 hours. The enriched biochar is finally packaged in plastic bags and stored in a refrigerator for subsequent use.

ISSN No:-2456-2165

C. Mixture design

A mixture design was chosen in order to obtain quality biochar. Table 1 gives the maximum and minimum percentages of the three components of the mixture. The lower and upper bounds of the proportions are chosen on the basis of the different expected performances of the biochar and after preliminary studies. The high proportion of sawdust in the composition of the mixture is justified by the fact that this lignocellulosic component is chosen as the major component. Rich in carbon, it could serve, after pyrolysis, as a depolluting agent. Carbon could be used incidentally also as a nutrient for plants. Clay is a second component; it can raise pH and the cation exchange capacity. Although the chicken manure is the third component, it will increase not only the nutrient content of the biochar but also its alkalizing effect.

Table 1: Lower and upper limits of the different components of the mixture

Components	Lower bound[%]	upper bound [%]
Sawdust powder from Ayous	50	55
Wak Clay Powder	20	30
Chicken manure's powder	15	20

D. Selected responses

The first response in this experimental design is the pH.Knowledge of the enriched biochar pH is a tool to evaluate its ability to reduce the acidity of the soil. The method of(Rajkovich et al., 2012) is used to measure the pH. The enriched biochar obtained from the various mixtures is suspended in distilled water, according to a liquid / solid ratio (L / S) of 20 ml / g. The pH measurement is carried out after stirring (1.5 hours) and using a portable pH meter (PCE-PHD 1).

The iodine index (I.I) is the second response of this experimental plan. It represents the measurement of the microporosity of the enriched biochar. The iodine number (in $mg.g^{-1}$) is the quantity in milligram of iodine adsorbed per gram of biochar enriched in an aqueous solution whose normality in iodine is 0.02 N according to AWWA B 600-78 (AWWA, 1991). In a 100 mL beaker, 0.2 g enriched biochar previously dried at 110 ° C for 24 h was introduced. A 20 ml solution of iodine (0.02 N) is added and the mixture is stirred for 30 min before filtration on filter paper. Ten (10) mL of the filtrate is taken and placed in an Erlenmeyer flask. From the burette, a solution of 0.1 N sodium thiosulphate is gradually added to the Erlenmeyer flask containing the filtrate until the solution is completely discolored. The iodine number is given by the following formula:

$$I.I(mg/g) = \frac{25,4x(20 - V_n)}{m_{ca}} \qquad (1)$$

With m_{cA} (g) the mass of enriched biochar, and V_n (ml) the volume of sodium thiosulfate at equilibrium.

Finally, the cationic exchange capacity (C.E.C.) is the last tested response on the enriched biochar obtained from the different mixtures. The cation exchange capacity is determined according to the standardized method AFNOR NFX 31-130 (AFNOR, 2000). The experimental setup consists of a 50 ml capacity glass column, inside which is installed a filtration device supporting a hydrophilic cotton. A mass of 2.5 g of enriched biochar is introduced into the column. The exchange sites of the enriched biochar are saturated by percolation with 75 mL of ammonium acetate (CH3COONH4, 1 $mol.L^{-1}$, pH = 7). The enriched biochar is then rinsed with 75 g of ethanol to remove excess ions. After drying at room temperature for 24 h, the sample is stirred in 50 mL NaCl (1 $mol.L^{-1}$) for 1 h. The solution of this stirring is then filtered on Wattman paper (N°1,) and the ammonium exchanged contained in this solution is measured spectrophotometrically at 600 nm.

E. Validation of response models

Validation of the models of the different responses is performed using the different statistical formulae: adjusted coefficient of determination (R^2 adjusted), absolute average deviation (AAD); the accuracy factor (A_f) and the bias factor (B_f). The formulae are represented by the following equations:

$$R^2 = \frac{\sum_{i=1}^{n}(y_{i,cal} - \bar{y})^2}{\sum_{i=1}^{n}(y_{i,\exp} - \bar{y})^2} \qquad (2)$$

$$AAD = \frac{\left[\sum_{n=1}^{n} \frac{\left(\left|y_{i\,\exp} - y_{i,\,cal}\right|\right)}{y_{i\,\exp}}\right]}{n} \qquad (3)$$

$$A_f = 10^{\frac{1}{n}\sum_{i=1}^{n}\left|\log\left(\frac{y_{i,cal}}{y_{i,\exp}}\right)\right|} \qquad (4)$$

$$Bf = 10^{\frac{1}{n}\sum_{i=1}^{n}\log\left(\frac{y_{i,cal}}{y_{i=1}}\right)} \qquad (5)$$

F. Optimization by the desirability function

One of the options for optimizing a process is the use of the desirability function (Del Castillo et al., 1996; Derringer and Suich, 1980; Harrington, 1965). The introduction of the desirability function was permitted to optimize the process of manufacturing enriched biochar. Individual desirability is calculated based on the maximization of each response. The global or composite desirability which represents the weighted geometric mean of individual desires. Individual desirability is calculated based on the maximization of each response according to the following equations:

$$d_i = 0 \qquad \hat{y} \prec L_i \qquad (6)$$

$$d_i = \left(\left(\hat{y}_i - L_i\right)/\left(T_i - L_i\right)\right)^i \qquad L_i \le \hat{y}_i \le T_i \qquad (7)$$

ISSN No:-2456-2165

$$d_i = 1 \qquad \hat{y} \prec T_i \tag{8}$$

with

$\hat{y}_i$ predicted value of the ith response;
T_i target value of the ith response;
L_i lowest acceptable value of the ith response;
d_i Desirability of the ith response;

The global or composite desirability which represents the weighted geometric mean of individual desirabilities(Vera Candioti et al., 2014). It is calculated according to the following formula:

$$D = \left(\prod \left(d_i^{W_i}\right)\right)^{\frac{1}{W}} \tag{9}$$

d_i Desirability of the ith response;
D desirability composite
w_i importance of the ith response;
W $\sum w_i$

G. Statistical analyzes

The mixing plan, the modeling and the optimization are carried using Minitab software, version 18.

III. RESULTS AND DISCUSSION

A. Analysis of the three responses

Table 2 presents the test matrix, associated responses and residue values. This table shows that the responses obtained are different for each experiment. This can lead to say that the different mixtures have different characteristics.

Table 2: Test matrix and associated responses

Trial	Reals values			Response			Residues		
	M1	M2	M3	pH	I.I	C.E.C.	pH	I.I	C.E.C.
N°	[g]	[g]	[g]		[mg.g^{-1}]	[cmol+.kg^{-1}]		[mg.g^{-1}]	[cmol+.kg^{-}]
1	50.00	31.25	18.75	9.52	768.00	41.0	0.09	1.8	-0.76
2	52.50	30.00	17.50	9.47	790.40	40.1	0.11	9.8	-1.21
3	50.00	35.00	15.00	8.66	766.37	37.7	0.01	-2.2	0.39
4	51.25	32.50	16.25	9.12	772.40	40.6	-0.12	-0.3	0.72
5	52.50	32.50	15.00	8.71	798.30	36.7	-0.00	5.8	0.47
6	51.25	31.25	17.50	9.40	771.40	40.9	-0.04	2.5	-0.63
7	51.25	33.75	15.00	8.7	770.00	35.0	0.00	-4.6	-1.78
8	53.75	31.25	15.00	8.78	820.33	35.2	0.15	-1.6	-0.42
9	51.25	30.00	18.75	9.34	762.00	41.1	-0.01	-0.9	-0.65
10	50.00	30.00	20.00	9.01	760.37	41.5	-0.05	-0.9	1.10
11	50.00	32.50	17.50	9.54	762.37	41.0	0.06	-6.5	-0.70
12	52.50	31.25	16.25	9.17	796.30	40.8	-0.01	8.8	1.31
13	53.75	30.00	16.25	9.05	802.47	40.2	-0.00	-11.5	1.14
14	55.00	30.00	15.00	8.38	866.33	34.5	-0.08	3.01	-0.48
15	51.67	31.67	16.67	9.25	761.40	41.2	-0.08	-13.5	0.72
16	50.00	33.75	16.25	9.20	780.33	41.0	-0.01	10.5	0.77

M1: *Ayous Sawdust's mass;* ***M2:*** *Wak clay's mass;* ***M 3:*** *Chicken manure's mass;*
pH.: *Hydrogen potential****;I.I.:*** *Iodine number;* ***C.E.C.:*** *Cation exchange capacity.*

The pH values of the various tests vary between 8.38 and 9.52, a variation of 11.22%. The biochar obtained after pyrolysis of all the different mixtures is basic. Although the alkaline character is found in most biochars derived from biomass of lignocellulosic origin(Anderson et al., 2021; Lange et al., 2018), this character seems to be reinforced in the presence of clay and chicken manure. These values are close to those obtained by (Chia Bhupinder et al., 2014) who mixed sawdust from Australia with different types of clay and poultry manure from this country. They are superior to those obtained by (Lange et al., 2018). This may be because their samples come only from sawdust from Canada. Iodine values range from 760.37 to 866.33 mg.g^{-1}, a variation of 6%. This variation is small compared to the variation in pH. This can be explained by the small variations in the proportions of the different components incorporated in the mixture design (variation of 3.75% for the mass of Ayous and Clay and 4% for the mass of chicken manure.Although the different components are subjected to pyrolysis, heat has little impact on the variations of the iodine index (POWAR and GANGIL, 2015). At moderate temperatures, the iodine index is thus weakly influenced (Tan et al., 2017; Zhong et al., 2012).

The cation exchange capacity of the tests varies between 34.5 and 41.5 cmol^{+} kg^{-1}, a variation of 20.28%.This variation is two to three times higher than the variation of pH and iodine value respectively. Thus, pyrolysis affects the cation exchange capacity more strongly than the other two responses studied (Lago et al., 2021); (Munera-Echeverri et al., 2018).

B. Validation of the models of the different answers

Table 3 presents the values of different quantities that were used to validate the model. Although the coefficients of determination for all responses are not greater than 95%, we can validate the model. This is justified by the fact that the other conditions are close to zero; even zero for the iodine value. The bias factor and the accuracy factor are also between 1 and 1.005.

Tableau 3: Model's validation

Response	Fitted R^2 [%]	AAD	B_f	Af_1
pH	92.85	0.02	1.02	1.02
I.I [$m^2.g^{-1}$]	90.81	0.000	1.00	1.00
CEC [cmol+.kg^-]	79.21	0.005	1.005	1.005

Fitted R^2= fitted Regression coefficient; AAD= Absolute average deviation; B_f= Biais factor; Af_1= Accuracy factor; pH.; I.I.: Iodine Index; C.E.C.: Cation exchange capacity.

C. Modelling the different response

- *Modelling the response "pH"*

The mathematical model resulting from the response (pH) is as follows:

$$pH = 8.46X_1 + 8.64X_2 + 9.02X_3 + 0.62X_1X_2 + 2.35X_1X_3 + 2.47X_2X_3 \quad (10)$$

This model is of quadratic type with interaction. It is noted that all the components taken alone positively influence the pH of the enriched biochar. The contribution of chickenmanure is higher, followed by that of clay (Table 3). This can be explained by the fact that, in general, chicken manureare basic and hens also peck mineral particles for digestion. Of most biomass type, chicken manure would have one of the most basic biochars (Lange et al., 2018). All interactions taken in pairs are also positive. Table 4 also presents the probability values and values of the variance inflation factor for pH. This table reveals that for the pH, the effect of all the constituents and the different interactions has a significant probability because less than 0.05 except the sawdust-clay interaction. The sawdust-clay interaction, however, is retained in the model at high contributions from sawdust and clay when evaluated separately. The variance inflation factor, which is between 2.35 and 2.42, also qualifies the experiment as fairly robust because the IVF is less than 10.

Table 4: Regression coefficients, p value and VIF ofpH

Componentsand interactions	Coeff.	p value	VIF
Sawdust =X1	8.46	0.000	2.42
Clay =X2	8.64	0.000	2.42
Chicken manure =X3	9.06	0.000	2.42
Sawdust* Clay =X1*X2	0.62	0.090	2.35
Sawdust*Chicken manure =X1*X3	2.35	0.000	2.35
Clay* Chicken manure = X2*X3	2.47	0.000	2.35

Coeff= coefficient; p=probability; VIF= Variance Inflation Factor

Figure 3 shows the pH mixing contour graph. Mixtures with a high pH are those rich in manure, followed by clay. The top of the triangle has compositions that are rich in sawdust but have a lower pH. The cox diagram (Fig. 4) associated with the mixing plane shows that overall the increase in pH is related to the increase in the proportion in chicken manure. This could be explained by the fact that the manure initially have a higher pH than the other components. The chicken manure is rich in nitrogen and minerals. This initial potentiality would also be less influenced by the pyrolysis temperature.

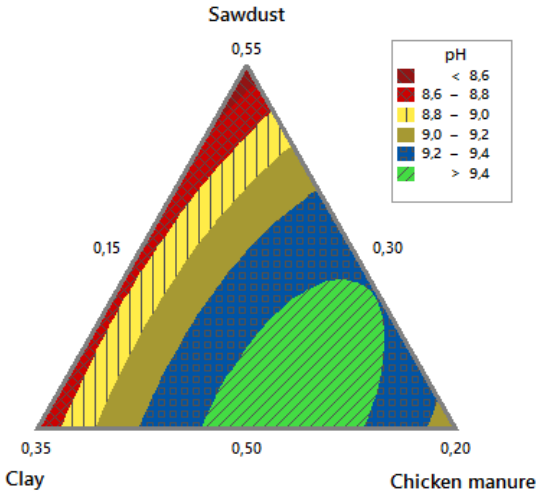

Fig. 3: Iso-response curveof pH

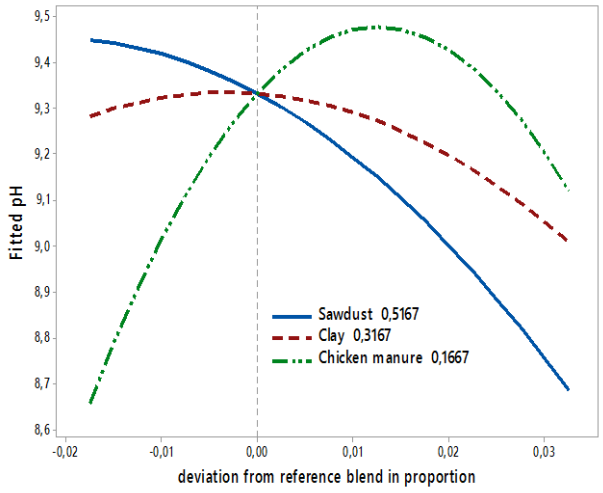

Fig. 4: Cox diagram on the pH of the components

D. Modelling the "Iodine Index" response

The mathematical model that follows from the analysis of the iodine index is as follows:

$$I.I = 863.32X_1 + 768.64X_2 + 761.28X_3 - 94.2X_1X_2 - 126.9X_1X_3 + 16X_2X_3 \quad (11)$$

For the iodine index, the model is quadratic with interaction. This model reveals that three components and clay-manure Interaction positively influence the iodine index. This is not the case for the sawdust-clay interaction and the sawdust-manure interaction.

Table 5 presents the evaluation of the regression coefficients for the iodine index. This table reveals that for the iodine index (I.I.), the effect of all the constituents and the sawdust-clay and sawdust-chicken manure interactions have a significant probability because the probability values p is less than 0.05. The clay-chicken manure interaction has a non-significant probability but remains important because of the significant influence of two components taken separately. The variance inflation factor, which is between 2.35 and 2.42, also qualifies the experiment as fairly robust because the VIF is less than 10.

Tableau 5:Regression coefficients, p value and VIF OF Iodine Index

Components and interactions	Coeff.	p value	VIF
Sawdust =X1	863.32	0.000	2.42
Clay =X2	768.64	0.000	2.42
Chicken manure =X3	761.28	0.000	2.42
Sawdust * Clay =X1*X2	-94.2	0.012	2.35
Sawdust*Chicken manure =X1*X3	-126.9	0.002	2.35
Clay* Chicken manure = X2*X3	16.0	0.616	2.35

Coeff= coefficient; p=probability; VIF= Variance Inflation Factor

Figure 5 shows the mixing contour graph of the iodine number (I.I.). High iodine number values are obtained when the mixture has a high sawdust composition. The other two components have an equal influence on iodine values. The cox diagram (Fig. 6) associated with the mixing plane shows that overall the increase in the proportion of sawdust increases the iodine number. This could be explained by the fact that the effect of the pyrolysis temperature, the component richest in carbon (here sawdust) reacts positively by developing micropores. This is not the case for chicken manure and clay.

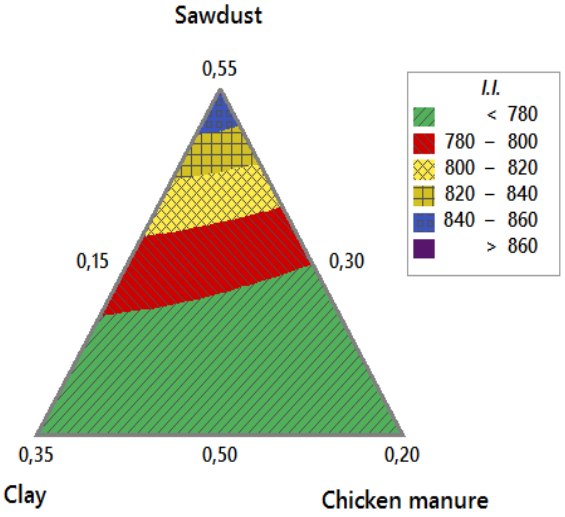

Fig. 5: Iso-response Curve of Iodine Index

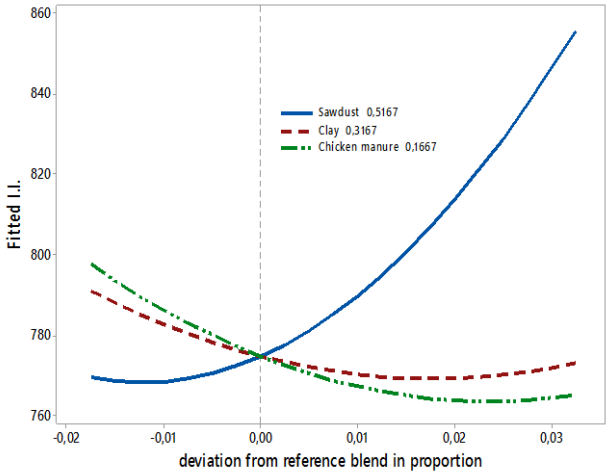

Fig. 6: Diagram of cox on the iodine index of the components

- *Modelling the response "Cation exchange capacity"*

The cation exchange capacity presents the following mathematical model:

$$C.E.C = 34.9X_1 + 36.36X_2 + 41.29X_3 + 4.43X_1X_2 + 16.12X_1X_3 + 4.26X_2X_3 \quad (12)$$

It is a mathematical model of quadratic type with three components and three interactions. This model reveals that sawdust, clay and chickenmanure and all interactions positively influence the cation exchange capacity. Of three components, manureis the components that strongly influence cation exchange capacity, followed by clay and sawdust. This can be explained by the fact that the manurecontains organic fractions close to the humins which have a high cation exchange capacity. If the influence of the clay is inferior to the manure, this can be explained by the type of clay used. Indeed, the clay of Wak is of kaolinite type. Kaolinite has only two layers and has a low cation exchange capacity compared to other types of clay. The three components associated during pyrolysis make it possible to obtain mixtures with a high cation exchange capacity because the three components interact in synergy.

ISSN No:-2456-2165

The sawdust-manure and clay-manure interactions act more strongly on the cation exchange capacity than the sawdust-clay interaction.

Table 6 shows that for the cation exchange capacity (CEC), the effect of all constituents and the sawdust-clay interaction have a significant probability because their probability values are less than 0.05. The sawdust-Clay and the clay-chicken interactions have a non-significant probability but remains important because of the significant influence of two components taken separately. The variance inflation factor, which is between 2.35 and 2.42, also qualifies the experiment as fairly robust because the VIF is less than 10.

Tableau 6: Regression coefficients, p value and VIF of the cation exchange capacity

Components and interactions	Coeff.	p value	VIF
Sawdust =X1	34.59	0.000	2.42
Clay =X2	36.36	0.000	2.42
Chicken manure =X3	41.29	0.000	2.42
Sawdust * Clay =X1*X2	4.43	0.368	2.35
Sawdust*Chicken manure =X1*X3	16.12	0.006	2.35
Clay* Chicken manure = X2*X3	4.26	0.386	2.35

Coeff= coefficient; p=probability; VIF= Variance Inflation Factor

Figure 7 shows the mixing contour graph of the cation exchange capacity (C.E.C). The cox diagram (Fig. 8) associated with the mixing plane shows that overall, the increase in the proportion in manure increases the cation exchange capacity. Rich in substance close to humins, chicken manure greatly increase the cation exchange capacity of enriched biochar.

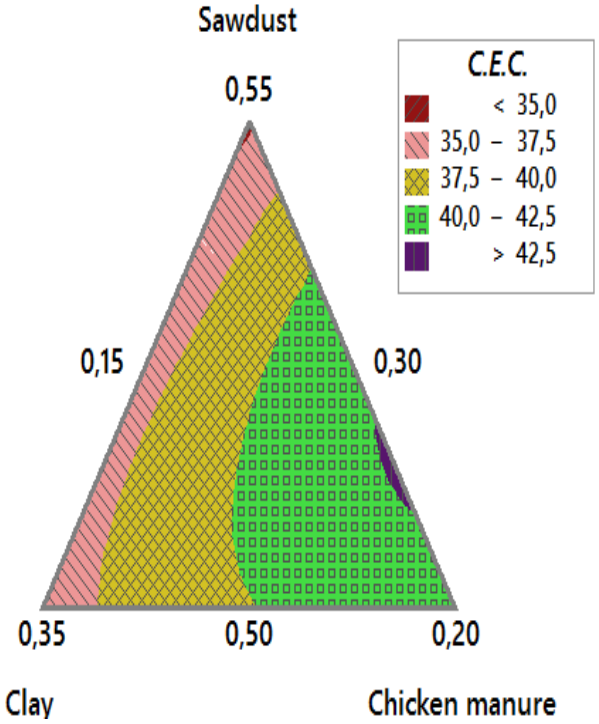

Fig. 7: CEC iso-response curve

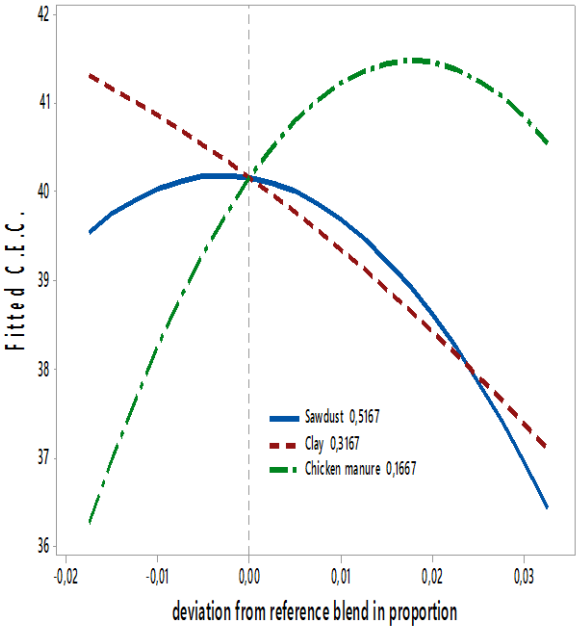

Fig. 8: Cox diagram on the CEC of the components

E. Identification of the optimal production zone of enriched biochar

The aim of this identification is to obtain an optimal zone. The overall optimization of the three responses can be done by superimposing the isometric response curves of the three constituents. Figure 9 shows the optimal zone (shown in white) and the non-optimal zone (shown in red). The optimal zone is the area where the goals of all three responses are achievable. The non-optimal zone is the area where, at least, one of the objectives of the three responses is not feasible.

ISSN No:-2456-2165

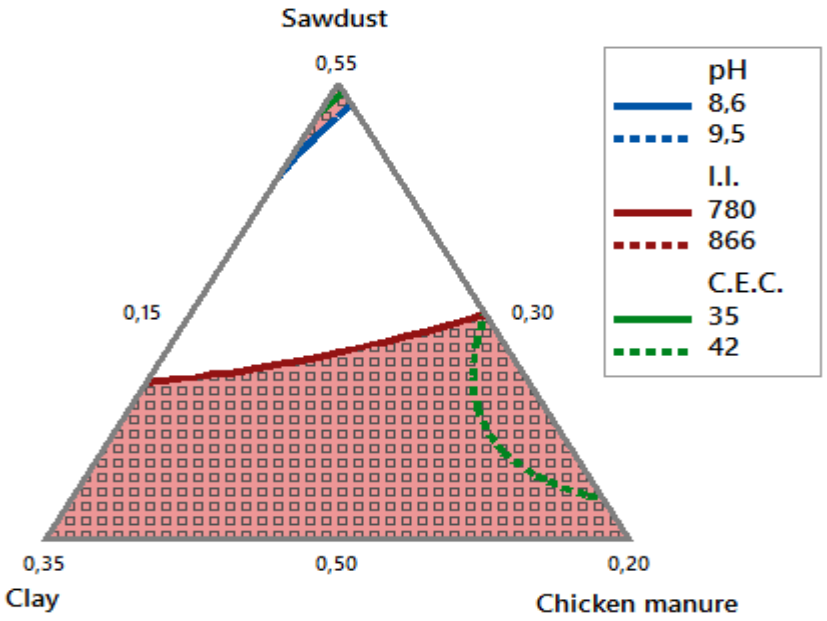

Fig. 9: Optimal (white) and non-optimal (dashed and red) zone of enriched biochar production

F. Optimization of the responses

Optimization of the responses was performed under the following conditions as shown in Table 7. If the weighting is the same for the three answers, this is not the case for the importance of the answers. We have tripled the importance of cation exchange capacity and doubled the importance of pH versus iodine value. Such a choice is justified by the fact that, intentionally, we want to obtain a biochar which in some cases can be used in the bioremediation of heavy metals in polluted soils and in other cases to be used as an amendment in poor soils. The low importance attributed to the iodine value is justified by the fact that it gives only an idea of the microporosity of the studied material. The choice of a very low weighting (0,1) is dictated by the fact that we want to attribute a low importance to the target of each response. This is in order to have a fairly large optimal area.

Table 7: Optimization conditions

Responses	Target	Low	target	Upper	Ponderation	Weight
pH	Maximum	8.46	9.06	9.06	0.1	2
I.I [$m^2.g^{-1}$]	Maximum	761	863	863	0.1	1
CEC [$cmol^+.kg^{-1}$]	Maximum	34.98	40.39	420	0.1	3

pH= Hydrogen potential; I.I.= Iodine Index; C.E.C.= Cation exchange Capacity.

One of the representation of the graphical optimization diagram is that of desirability(Bezerra et al., 2008; Myers, R.H,; Montgomery, 2009). The optimization diagram illustrates the effect of each response on the average geometric deviations (Figure 10). The bold and dashed vertical lines and the corresponding (bracketed) values indicate the optimal component levels. The horizontal lines (in bold and in solid lines) and the values of the answers (denoted y) correspond to the average geometric deviations compared to the levels of the optimal components found.

ISSN No:-2456-2165

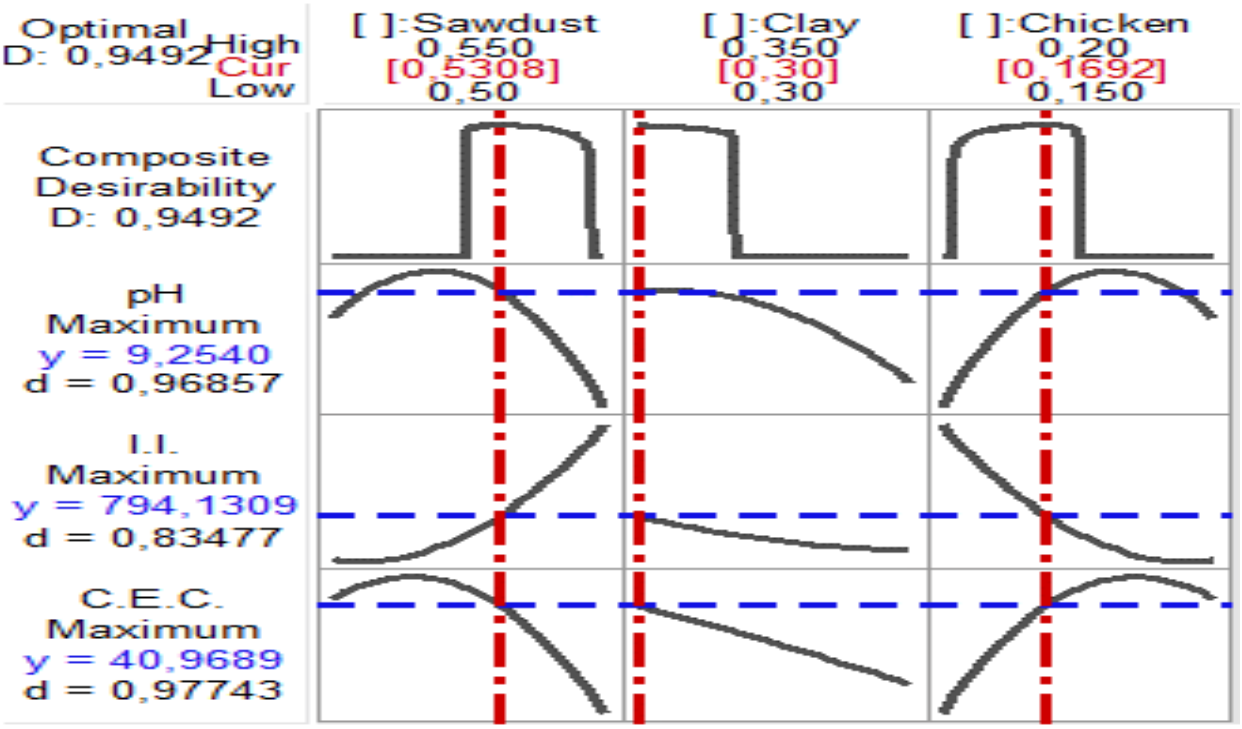

Fig. 10: Optimization diagram by the desirability function

Desirability values are 0.96 for pH, 0.83 for iodine value and 0.97 for cation exchange capacity. These values are close to 1, except for the desirability value of the iodine number. The composite desirability is 0.94 and is close to 1. This indicates that the components appear to achieve favorable results for all responses as a whole. The composite desirability is greater than the individual desirability of the iodine value. Indeed, we have tripled the importance of the cation exchange capacity and doubled the importance of the pH compared to the iodine index. Of all the responses, the components are more efficient at maximizing the cation exchange capacity than for the other two responses. This can be explained by the fact that there is a synergetic effect and that the clay powders and hog manure agglomerate effectively on the sawdust.

IV. CONCLUSION

The different proportions of components and their chemical composition make it possible to obtain different responses from the enriched biochar. The components as well as most of the interactions are possible on the responses studied except the microporosity. The desirability function allows the optimal composition of the various constituents of the enriched biochar. Enriched biochar implementations on soils polluted with heavy metals or on poor soils are necessary to appreciate the proposed biochar.

ACKNOWLEDGMENT

We thank the special fund of support for the modernization of research of the Ministry of Higher Education of Cameroon and the University of Ngaoundere, which allowed us the feasibility of this study.

REFERENCES

[1.] Adjia, Fezeu, Tchatchueng, Sorho, Echevarria, Ngassoum, 2009. Long term effect of municipal solid waste amendment on soil heavy metal content of sites used for periurban agriculture in Ngaoundere, Cameroon. J. Environ. Sci. 2, 412–421.

[2.] AFNOR, 2000. AFNOR NFX 31-130. Soils quality - Chemical methods - Determination of cationic exchange capacity (CEC) and extracible cations.

[3.] Anderson, N., Gu, H., Bergman, R., 2021. Comparison of novel biochars and steam activated carbon from mixed conifer mill residues. Energies 14, 1–19. https://doi.org/10.3390/en14248472

[4.] AWWA, 1991. AWWA Standart of power activated carbon AWWA B 600-90.

[5.] Belibi Belibi, P.D., 2016. Mise au point d'une membrane céramique de microfiltration à base de matériau argileux du Cameroun: Application à l'élimination de la kaolinte des eaux de consommation.

[6.] Bezerra, M.A., Santelli, R.E., Oliveira, E.P., Villar, L.S., Escaleira, L.A., 2008. Response surface methodology (RSM) as a tool for optimization in analytical chemistry. Talanta 76, 965–977. https://doi.org/10.1016/j.talanta.2008.05.019

[7.] Blackwell, P., Joseph, S.D., Anawar, H.M., 2015. Influences of Biochar and Biochar-Mineral Complex on Mycorrhizal Colonisation and Nutrition of Wheat and Sorghum. https://doi.org/10.1016/S1002-0160(15)30049-7

[8.] Blackwell, P., Krull, E., Butler, G., Herbert, A., Solaiman, Z., 2010. Effect of banded biochar on dryland wheat production and fertiliser use in south-western Australia: An agronomic and economic perspective. Aust. J. Soil Res. 48, 531–545. https://doi.org/10.1071/SR10014

[9.] Chan, K.Y., Zu, Z., 2009. Biochar: nutriment properties and their enchancement, in: Earth-scan (Ed.), Biochar for Environmental Management: Science and Technology. London, pp. 67–84.
[10.] Chen, X., Chen, G., Chen, L., Chen, Y., Lehmann, J., McBride, M.B., Hay, A.G., 2011. Adsorption of copper and zinc by biochars produced from pyrolysis of hardwood and corn straw in aqueous solution. Bioresour. Technol. 102, 8877–8884. https://doi.org/10.1016/j.biortech.2011.06.078
[11.] Cheng, C.H., Lehmann, J., 2009. Ageing of black carbon along a temperature gradient. Chemosphere 75, 1021–1027. https://doi.org/10.1016/j.chemosphere.2009.01.045
[12.] Chia Bhupinder, C.H., Singh, P., Joseph, Stephen, Graber, Ellen R, Munroe, Paul, Chia, C H, Singh, B P, Joseph, S, Graber, E R, Munroe, P, Chia, Chee H, Singh, Bhupinder Pal, 2014. Title: Characterization of an Enriched Biochar Characterization of an Enriched Biochar. J. Anal. Appl. Pyrolysis. https://doi.org/10.1016/j.jaap.2014.05.021
[13.] Clare, A., Shackley, S., Joseph, S., Hammond, J., Pan, G., Bloom, A., 2015. Competing uses for China's straw: The economic and carbon abatement potential of biochar. GCB Bioenergy 7, 1272–1282. https://doi.org/10.1111/gcbb.12220
[14.] Del Castillo, E., Montgomery, D.C., McCarville, D.R., 1996. Modified desirability functions for multiple response optimization. J. Qual. Technol. 28, 337–345. https://doi.org/10.1080/00224065.1996.11979684
[15.] Derringer, G., Suich, R., 1980. Simultaneous Optimization of Several Response Variables. J. Qual. Technol. 12, 214–219. https://doi.org/10.1080/00224065.1980.11980968
[16.] Fezeu Wombuwou, M.L., 2006. Statut minéral des sols, des plantes des eaux d'abreuvage et de bovins du pâturage de Wakwa au Cameroun.
[17.] Glaser, B., Haumaier, L., Guggenberger, G., Zech, W., 2001. The "Terra Preta" phenomenon: A model for sustainable agriculture in the humid tropics. Naturwissenschaften 88, 37–41. https://doi.org/10.1007/s001140000193
[18.] Harrington, F.C., 1965. The Desirabilty function. Industrial Quality Control 21.
[19.] Hassana, B., Mbawala, A., Ngassoum, M., Ibrahima, A., 2019. Etude de la disponibilité de quelques résidus de biomasse en vue de leur transformation en biochar: cas de la ville de Ngaoundéré (Cameroun). Int. Multiling. J. Sci. Technol. 4, 2528–9810.
[20.] Joseph, S., Anawar, H.M., Storer, P., Blackwell, P., Chia, C., Lin, Y., Munroe, P., Donne, S., Horvat, J., Wang, J., Solaiman, Z.M., M, A.H., M, S.Z., 2015. Effects of Enriched Biochars Containing Magnetic Iron Nanoparticles on Mycorrhizal Colonisation, Plant Growth, Nutrient Uptake and Soil Quality Improvement, Pedosphere. https://doi.org/10.1016/S1002-0160(15)30056-4
[21.] Joseph, S., Graber, E.R., Chia, C., Munroe, P., Donne, S., Thomas, T., Nielsen, S., Marjo, C., Rutlidge, H., Pan, G.X., Li, L., Taylor, P., Rawal, A., Hook, J., 2013. Shifting paradigms: Development of high-efficiency biochar fertilizers based on nano-structures and soluble components. Carbon Manag. 4, 323–343. https://doi.org/10.4155/cmt.13.23
[22.] Joseph, S.D., Camps-Arbestain, M., Lin, Y., Munroe, P., Chia, C.H., Hook, J., Van Zwieten, L., Kimber, S., Cowie, A., Singh, B.P., Lehmann, J., Foidl, N., Smernik, R.J., Amonette, J.E., 2010. An investigation into the reactions of biochar in soil. Aust. J. Soil Res. 48, 501–515. https://doi.org/10.1071/SR10009
[23.] Kimetu, J.M., Lehmann, J., Ngoze, S.O., Mugendi, D.N., Kinyangi, J.M., Riha, S., Verchot, L., Recha, J.W., Pell, A.N., 2008. Reversibility of soil productivity decline with organic matter of differing quality along a degradation gradient. Ecosystems 11, 726–739. https://doi.org/10.1007/s10021-008-9154-z
[24.] Lago, B.C., Silva, C.A., Melo, L.C.A., Morais, E.G. de, 2021. Predicting biochar cation exchange capacity using Fourier transform infrared spectroscopy combined with partial least square regression. Sci. Total Environ. 794. https://doi.org/10.1016/j.scitotenv.2021.148762
[25.] Lange, S., Allaire, D., Charles, A., Auclair, I., CE, B., 2018. Propriétés physicochimiques de 43 biochars 60.
[26.] Li, Y., Wang, Z., Xie, X., Zhu, J., Li, R., Qin, T., 2017. Removal of Norfloxacin from aqueous solution by clay-biochar composite prepared from potato stem and natural attapulgite. Colloids Surfaces A Physicochem. Eng. Asp. 514, 126–136. https://doi.org/10.1016/j.colsurfa.2016.11.064
[27.] Li, Yongfu, Hu, S., Chen, J., Müller, K., Li, Yongchun, Fu, W., Lin, Z., Wang, H., 2018. Effects of biochar application in forest ecosystems on soil properties and greenhouse gas emissions: a review. J. Soils Sediments 18, 546–563. https://doi.org/10.1007/s11368-017-1906-y
[28.] Liang, B., Lehmann, J., Solomon, D., Kinyangi, J., Grossman, J., O'Neill, B., Skjemstad, J.O., Thies, J., Luizão, F.J., Petersen, J., Neves, E.G., 2006. Black Carbon Increases Cation Exchange Capacity in Soils. Soil Sci. Soc. Am. J. 70, 1719–1730. https://doi.org/10.2136/sssaj2005.0383
[29.] Munera-Echeverri, J.L., Martinsen, V., Strand, L.T., Zivanovic, V., Cornelissen, G., Mulder, J., 2018. Cation exchange capacity of biochar: An urgent method modification. https://doi.org/10.1016/j.scitotenv.2018.06.017
[30.] Myers, R.H,; Montgomery, D.., 2009. Response Surface Methodology: Process and Product Optimization Using Designed Experiments. Wiley Series in Probalility and Statistics, Wiley New York.
[31.] Noubissié, E., Ngassoum, M.B., Ali, A., Castro-Georgi, J., Donard, O.F.X., 2016. Contamination of market garden soils by metals (Hg, Sn, Pb) and risk for vegetable consumers of Ngaoundéré (Cameroon). Euro-Mediterranean J. Environ. Integr. 1. https://doi.org/10.1007/s41207-016-0009-2
[32.] Pan, H., Yang, X., Chen, H., Sarkar, B., Bolan, N., Shaheen, S.M., Wu, F., Che, L., Ma, Y., Rinklebe, J., Wang, H., 2021. Pristine and iron-engineered animal- and plant-derived biochars enhanced bacterial abundance and immobilized arsenic and lead in a contaminated soil. Sci. Total Environ. 763, 144218. https://doi.org/10.1016/j.scitotenv.2020.144218

[33.] POWAR, R.V., GANGIL, S., 2015. Effect of temperature on iodine value and total carbon contain in bio-char produced from soybean stalk in continuous feed reactor. Int. J. Agric. Eng. 8, 26–30. https://doi.org/10.15740/has/ijae/8.1/26-30
[34.] Rajkovich, S., Enders, A., Hanley, K., Hyland, C., Zimmerman, A.R., Lehmann, J., 2012. Corn growth and nitrogen nutrition after additions of biochars with varying properties to a temperate soil. Biol. Fertil. Soils 48, 271–284. https://doi.org/10.1007/s00374-011-0624-7
[35.] Rumaizah, C.Z., Fazureen, A., Mohd Hasmizam, R., Asmadi, A., Mohd Al Amin, M.N., 2019. Properties and filtration performance of porous clay membrane produced using sawdust as pore forming agent. Key Eng. Mater. 821 KEM, 337–342. https://doi.org/10.4028/www.scientific.net/KEM.821.337
[36.] Sun, H., Zhang, Y., Yang, Y., Chen, Y., Jeyakumar, P., Shao, Q., Zhou, Y., Ma, M., Zhu, R., Qian, Q., Fan, Y., Xiang, S., Zhai, N., Li, Y., Zhao, Q., Wang, H., 2021. Effect of biofertilizer and wheat straw biochar application on nitrous oxide emission and ammonia volatilization from paddy soil. Environ. Pollut. 275, 116640. https://doi.org/10.1016/j.envpol.2021.116640
[37.] Tan, Z., Wang, Y., Kasiulienė, A., Huang, C., Ai, P., 2017. Cadmium removal potential by rice straw-derived magnetic biochar. Clean Technol. Environ. Policy 19, 761–774. https://doi.org/10.1007/s10098-016-1264-2
[38.] Vera Candioti, L., De Zan, M.M., Cámara, M.S., Goicoechea, H.C., 2014. Experimental design and multiple response optimization. Using the desirability function in analytical methods development. Talanta 124, 123–138. https://doi.org/10.1016/j.talanta.2014.01.034
[39.] Wang, B., Gao, B., Fang, J., 2017. Recent advances in engineered biochar productions and applications. Crit. Rev. Environ. Sci. Technol. 47, 2158–2207. https://doi.org/10.1080/10643389.2017.1418580
[40.] Yang, X., Pan, H., Shaheen, S.M., Wang, H., Rinklebe, J., 2021. Immobilization of cadmium and lead using phosphorus-rich animal-derived and iron-modified plant-derived biochars under dynamic redox conditions in a paddy soil. Environ. Int. 156. https://doi.org/10.1016/j.envint.2021.106628
[41.] Yao, Y., Gao, B., Fang, J., Zhang, M., Chen, H., Zhou, Y., Creamer, A.E., Sun, Y., Yang, L., 2014. Characterization and environmental applications of clay-biochar composites. Chem. Eng. J. 242, 136–143. https://doi.org/10.1016/j.cej.2013.12.062
[42.] Zhong, Z.Y., Yang, Q., Li, X.M., Luo, K., Liu, Y., Zeng, G.M., 2012. Preparation of peanut hull-based activated carbon by microwave-induced phosphoric acid activation and its application in Remazol Brilliant Blue R adsorption. Ind. Crops Prod. 37, 178–185. https://doi.org/10.1016/j.indcrop.2011.12.015.